PHYSICAL REVIEW B VOLUME 51, NUMBER 2 1 JANUARY 1995-II

Squeezed excited states in exciton-phonon systems

Mathias Sonnek, Hubert Eiermann, and Max Wagner
Institut für Theoretische Physik, Universität Stuttgart, Pfaffenwaldring 57, 70550 Stuttgart, Germany

(Received 12 September 1994)

In earlier work unusual excited exciton-phonon states have been found for prototype exciton-phonon Hamiltonians (dimer, trimer). These states have been calculated numerically by diagonalizing the respective Fulton-Gouterman equations. Their physical character is such that the motion of the effective exciton becomes free whereas in the vibrational subspace the dynamics is governed by an effective stiffening of the nearest-neighbor interaction. In the present work it is shown analytically by means of a Fröhlich-type transformation, how the stiffening in the phonon dynamics is generated, such that the phononic part for these nonconventional exciton-phonon states is well described by squeezed oscillatory functional forms.

I. INTRODUCTION

The experimental background motivation for the present and also for preceding work was the phenomenon of retarded luminescence which has been found both in rare-gas crystals[1] and in alkali halides.[2] The conventional theoretical description of this phenomenon is provided by the so-called "barrier model" of self-trapping, originally proposed by Rashba[3] and Toyozawa.[4] This model relies heavily on the adiabatic approximation and, as shown in earlier work,[5] leads to divergence problems, if nonadiabatic terms are included. To avoid these problems an alternate type of concept has been introduced[6,7] which is based on the use of the Fulton-Gouterman transformation. The dominant favorable quality of this concept is the fact that it leads to the diagonalization of the excitonic (electronic) subspace. In this manner Schrödinger-like equations for the vibrational subspace are derived, which are of nonharmonic nature, but are well-suited for computational handling. Moreover these Fulton-Gouterman equations display the fundamental two antagonistic tendencies inherent in each exciton-phonon dynamics in a highly suggestive way, such that the analytic character of the vibrational wave functions is elucidated. This type of analysis in earlier work has yielded an unusual type of excited exciton-phonon states,[8] which followed from a numerical diagonalization of the Fulton-Gouterman equations. The most pronounced feature of these solutions with regard to the vibrational part $|\phi(Q)\rangle$ of the wave function (Q = vibrational coordinate) is their compressed, practically undisplaced form ("squeezed states") indicating a liberation from its tendency to self-trapping. The aim of the present paper is to understand the numerically found unusual excited states in an analytic manner.

The basic frame of the present work will be the Fulton-Gouterman transformation. The evolving Fulton-Gouterman Hamiltonian in the vibrational subspace is handled by three different sequences of unitary transformations. In the first of these three approaches a product of unitary transformations aims at simulating the dominant antagonistic tendencies[9,10] in the Fulton-Gouterman (FG) Hamiltonian. In the second approach a Fröhlich-type transformation[11] is used for a further transcription of the FG Hamiltonian which then displays a squeezed nature in the phononic subspace. By means of this, direct analytical evidence is given that squeezed oscillatory solutions pertain to this transformed Hamiltonian. A deficiency of the Fröhlich-type transformation is that the transformed Hamiltonian cannot be written down in a closed form. This can be overcome by the third sequence of transformations, which is deduced from the Fröhlich approach.

In Sec. II we introduce the model Hamiltonian and the FG transformation. In Secs. III–V the three aforementioned sequences of unitary transformations are discussed. Section VI presents the description of the states within the Born-Oppenheimer approximation. Finally, we close the paper in Sec. VII with a summary.

II. BACKGROUND: THE FULTON-GOUTERMAN TRANSFORMATION (DIMER)

We consider an archetype exciton-phonon model (dimer, two-site model) characterized by the Hamiltonian

$$H=\frac{\Omega}{2}\{(P^2+Q^2)-T\cdot(|l\rangle\langle r|+|r\rangle\langle l|)+D\cdot Q\cdot(|l\rangle\langle l|-|r\rangle\langle r|)\}\ , \tag{1}$$

where T represents the excitonic transfer and D the exciton-phonon coupling constants. This model has been considered by Shore and Sander,[12] who used the Fulton-Gouterman transformation (FGT) to calculate the ground state. Later many other researchers have discussed this model.

We introduce the unitary operator

$$U_{\text{FG}}=\frac{1}{\sqrt{2}}\sum_p\{[|l\rangle+p|r\rangle R_Q]\langle p|\}\ , \tag{2}$$

where R_Q is the reflection operator in Q space, $R_Q Q=-QR_Q$, $R_Q|\phi(Q)\rangle=|\phi(-Q)\rangle$, and p denotes the parity $p=\pm 1$. Then the fundamental transformation properties of $T_{\mathrm{FG}}: A=U_{\mathrm{FG}}^{\dagger} A U_{\mathrm{FG}}$, $T_{\mathrm{FG}}: |\Psi\rangle = U_{\mathrm{FG}}^{\dagger} |\Psi\rangle$ are given by

$$\begin{aligned}
&T_{\mathrm{FG}}:(|l\rangle\langle r|+|r\rangle\langle l|)=\sum_p p|p\rangle\langle p|R_Q ,\\
&T_{\mathrm{FG}}:(|l\rangle\langle r|-|r\rangle\langle l|)=\sum_p p|-p\rangle\langle p|R_Q ,\\
&T_{\mathrm{FG}}:(|l\rangle\langle l|-|r\rangle\langle r|)=\sum_p |-p\rangle\langle p| ,\\
&T_{\mathrm{FG}}:Q=\sum_p |-p\rangle\langle p|Q ,\\
&T_{\mathrm{FG}}:P=\sum_p |-p\rangle\langle p|P ,\\
&T_{\mathrm{FG}}:\frac{1}{\sqrt{2}}(|l\rangle|f(Q)\rangle+p|r\rangle R_Q|f(Q)\rangle)=|p\rangle|f(Q)\rangle .
\end{aligned} \tag{3}$$

The operators Q^2 and P^2 remain unaltered ($T_{\mathrm{FG}}:Q^2=Q^2$, $T_{\mathrm{FG}}:P^2=P^2$).

The Hamiltonian (1) is diagonalized by T_{FG} with respect to the parity states $|p\rangle$ in the excitonic subspace (FGT):

$$T_{\mathrm{FG}}:H=U_{\mathrm{FG}}^{\dagger} H U_{\mathrm{FG}}=\sum_p |p\rangle\langle p|H_{\mathrm{FG}}^{(p)}(Q,P) . \tag{4}$$

In this manner the problem is reduced to the solution of Schrödinger-like equations (FG equations) of the form $H_{\mathrm{FG}}^{(p)}|\phi_n^{(p)}\rangle = E_n^{(p)}|\phi_n^{(p)}\rangle$ or

$$\frac{\Omega}{2}\left[P^2+Q^2+\underbrace{DQ}_{\substack{\text{self-trapping}\\ \text{tendency}}}-\underbrace{pTR_Q}_{\substack{\text{anti-self-trapping}\\ \text{tendency}}}\right]|\phi_n^{(p)}(Q)\rangle = E_n^{(p)}|\phi_n^{(p)}(Q)\rangle . \tag{5}$$

The total wave function of the original Hamiltonian then reads

$$\begin{aligned}
|\Psi_n^{(p)}\rangle &= U_{\mathrm{FG}}|p\rangle|\phi_n^{(p)}\rangle\\
&=\frac{1}{\sqrt{2}}[|l\rangle|\phi_n^{(p)}\rangle+p|r\rangle R_Q|\phi_n^{(p)}\rangle] .
\end{aligned} \tag{6}$$

The Fulton-Gouterman Hamiltonian exhibits two antagonistic tendencies ("displacement" and "reflection" or likewise "self-trapping" and "anti-self-trapping"), which in their counteraction generate different species of wave functions in different energy regions.

The global picture of the eigenfunctions and energies, as found by numerical diagonalization of the FG equations (5), is shown in Figs. 1 and 2. In Fig. 1, to spare

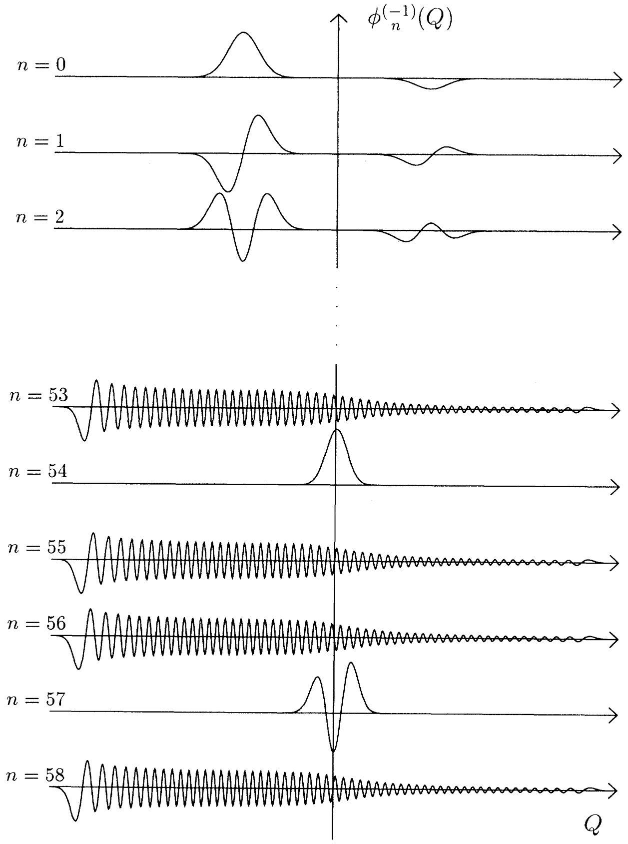

FIG. 1. Eigenfunctions of the FG equation (5) for $p=-1$, $D=15$, $T=50$. All functions below $n=54$ display an odd number of nodes, whereas the eigenfunctions $n=54$ and $n=57$ display an even number of nodes.

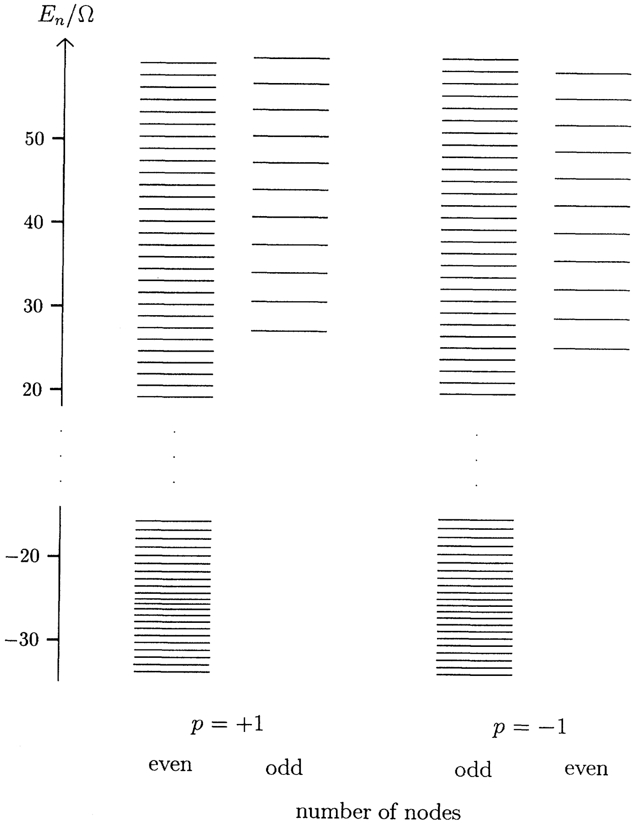

FIG. 2. Energetic arrangement of eigenstates of $D=15$ and $T=50$. lhs: parity $p=+1$, rhs: $p=-1$.

space, we present only the vibrational wave functions $|\phi_n^{(-1)}(Q)\rangle$ pertaining to the odd parity case $(p=-1)$ where the terminus "odd" is fixed by the convention that the bare excitonic site functions $|l\rangle$ and $|r\rangle$ are assumed to be of even nature

$$R_{\text{ex}}|l\rangle=|r\rangle\ ,\quad R_{\text{ex}}|r\rangle=|l\rangle\ , \tag{7}$$

(R_{ex}: excitonic reflection operator). If we had chosen the bare exciton functions to be of odd parity, $R_{\text{ex}}|l\rangle=-|r\rangle$, $R_{\text{ex}}|r\rangle=-|l\rangle$, which actually corresponds to the situation in rare-gas crystals, the sign in front of the T term in the FG equations (5) would be reversed, which would amount also in a reversal of the parity assignments of the vibrational wave functions.[8]

From Fig. 1 we note that there are two different species of vibrational wave functions. For lower quantum numbers the dominant part of $|\phi_n^{(p)}(Q)\rangle$ exhibits a displacement in Q space. This displacement reflects the self-trapping tendency of the FG equations, since it indicates the displaced atomic structure. The displaced dominant part of the vibrational wave function is supplemented by a mirror image of diminished weight, which reflects the anti-self-trapping tendency of the FG equations and partially liberates the exciton from its elastic encasement. Taken together, both parts of $|\phi_n^{(p)}(Q)\rangle$ represent an effective broadening of the total extension of $|\phi_n^{(p)}\rangle$ in Q space ("antisqueezing"). However, for strong exciton-oscillator coupling values $(T/D \ll 1)$, one should remain aware of the disintegration of the vibrational wave function into two parts located in different spatial areas.[10] For dominating excitonic transfer $(T/D \gg 1)$, on the other hand, both maxima merge together into a single structural form located near the undisplaced equilibrium position $Q=0$. In this manner one indeed would have a broadened form of the wave function.

For higher quantum numbers another type of vibrational wave functions makes its appearance. For the chosen parameter pair of Figs. 1 and 2 $(D=15,\ T=50)$ the lowest of these states appears for the quantum number $n=54$. We note that these unconventional types of states display functional forms which again start with a small number of nodes. They practically do not exhibit a displacement of the oscillatory equilibrium. Also, compared to the corresponding vibrational forms of the uncoupled oscillator, their spatial extension turns out to be reduced (squeezing). In addition we observe that the functional forms of the vibrational states in the energetic neighborhood of the unconventional states are of strongly extended nature with a high number of nodes.

In total, the node arrangement of the two types of vibrational wave functions is very peculiar. For the chosen example of odd parity $(p=-1)$ the conventional, i.e., the self-trapped, states have an odd number of nodes, whereas those in the series of nonconventional states have an even number. For even parity $(p=+1)$ the situation is just reversed.

In Fig. 2 the respective sequences of states are shown in their energetic arrangement. It turns out that the conventional states generally have an energetic spacing which for the chosen parameter pair is close to the undisturbed decoupled oscillator, whereas for the unconventional states the spacing is distinctively larger.

In Fig. 3 the overall behavior of the eigenstates for a given transfer parameter T and $p=-1$ is shown in its dependence on the coupling value D. The conventional states are those attached to the descending lines whereas the nonconventional ones pertain to the ascending lines. In those regions where two lines come close together and display a strong curvature, a clear distinction between the two types of states no longer is possible. In passing we note that similar results were found by Reik for related systems.[13]

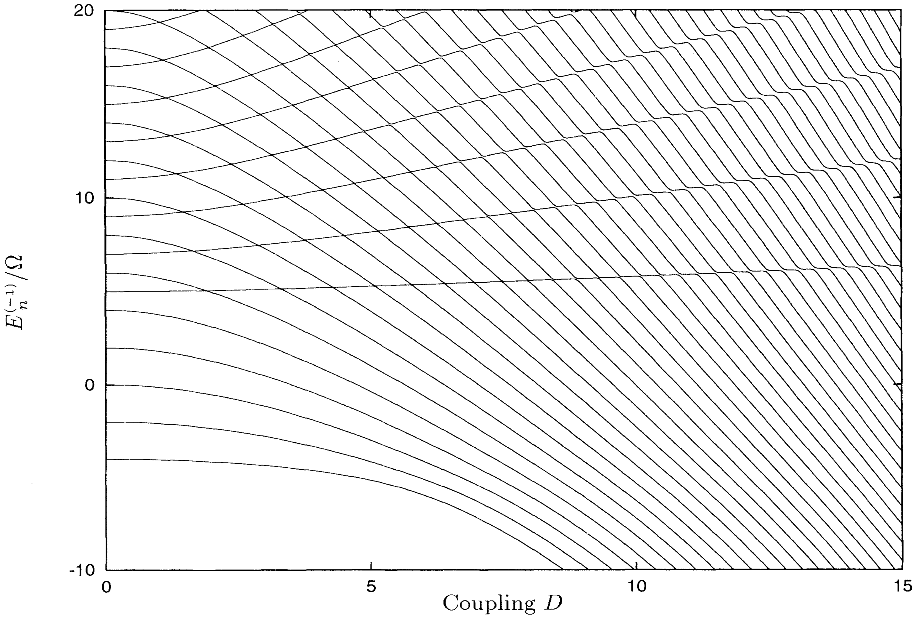

FIG. 3. Dependence of the energy eigenvalues on the coupling D for $p=-1$, $T=10$. The descending lines pertain to the conventional states, the ascending lines to the nonconventional states.

III. UNITARY GENERATION OF SQUEEZED DISPLACED TRIAL FUNCTIONS

Motivated by the numerical finding of the peculiar excited states given in Fig. 1 and in Ref. 8, we now attempt to obtain an analytical justification for the unconventional behavior. This is most easily achieved by means of unitary transformations. In considering the spatial form of the numerically found unconventional vibrational wave functions, it would seem suggestive to use a product of unitary transformations with one constituent producing an effective squeezing of the vibrational wave functions, whereas the other constituent could account for the residual small displacement. Realizing this philosophy we introduce the two unitary operators

$$U_d=e^{S_d}\ ,\quad S_d=idP\ , \tag{8}$$

$$U_s=e^{S_s}\ ,\quad S_s=-is(PQ+QP)\ . \tag{9}$$

We assume that the unitary product transformation $\tilde{H}^{(p)}_{\mathrm{FG}}=(U_sU_d)^{\dagger}H^{(p)}_{\mathrm{FG}}(U_sU_d)$ establishes a Hamiltonian which in its effective dynamics is represented by an undisturbed oscillator Hamiltonian in the respective energy regime of the unconventional states. For the odd parity case $p=-1$, its ground state then would be given approximately by that of the uncoupled oscillator

$$\tilde{\phi}^{(-1)}_{\mathrm{FG}}(Q)\approx\phi_0(Q)=\pi^{-1/4}\exp(-Q^2/2)\ . \tag{10}$$

This, inversely, would mean that the lowest state is approximated by

$$\phi^{(-1)}_{\mathrm{FG}}(Q)=U_sU_d\tilde{\phi}^{(-1)}_{\mathrm{FG}}(Q)\approx U_sU_d\phi_0(Q)\ . \tag{11}$$

We consider this form as a trial wave function depending on the parameters s and d of the two unitary operators (8) and (9). The unitary transformation operators (8) and (9) have the properties

$$U_df(Q)=f(Q+d)\ , \tag{12}$$

$$U_sf(Q)=e^{-s}f(e^{-2s}Q)\ . \tag{13}$$

Specifically, if we apply the product of operators onto $\phi_0(Q)$, we obtain

$$\phi^{(-1)}_{\mathrm{FG}}(Q)\approx\pi^{-1/4}e^{-s}\exp[-1/2(e^{-2s}Q+d)^2]$$
$$\equiv\phi(d,s)\ . \tag{14}$$

For further details about unitary transformations we refer to a book by one of us.[14] Taking a glance at the structural form of the right-hand side (rhs) of Eq. (14) we note that indeed it is of a squeezed, displaced Gaussian type which may be assumed to yield a good simulation of the lowest unconventional state ($n=54$ of Fig. 1). The two transformation parameters d and s are fixed by employing the trial wave function $\phi(d,s)$, given in (14), in an optimization procedure. As a variational principle we adopt the minimization of the squared variance of the energetic expectation value

$$\delta(\langle\phi|H^{(-1)2}_{\mathrm{FG}}|\phi\rangle-\langle\phi|H^{(-1)}_{\mathrm{FH}}|\phi\rangle^2)=0\ . \tag{15}$$

For this variance we find

$$\langle\phi|H^{(-1)2}_{\mathrm{FG}}|\phi\rangle-\langle\phi|H^{(-1)}_{\mathrm{FG}}|\phi\rangle^2$$
$$=\Omega^2\left\{\frac{T^2}{4}(1-e^{-2d^2})+\frac{T}{2}de^{-d^2}[De^{2s}-2d\cosh(4s)]+\frac{1}{2}\sinh^2(4s)+\frac{1}{8}e^{4s}(D-2de^{2s})^2\right\}\ . \tag{16}$$

Applying the variation with respect to the two parameters d and s we find two equations which we refrain from writing down explicitly. These two equations fix the two parameters d and s as functions of the intrinsic material constants D and T of the original Hamiltonian. The result is shown in Figs. 4 and 5. The magnitude of both the displacement parameter d and the squeezing parameter s increases with a growing exciton-oscillator interaction constant D and decreases with an enhanced excitonic transfer rate T. The limiting analytical behavior of d and s for $D\ll(T-1)$ reads

$$d=-\frac{1}{2}\cdot\frac{D}{T-1}+\frac{T}{16}\left[\frac{D}{T-1}\right]^3+O\left[\left[\frac{D}{T-1}\right]^5\right]\ , \tag{17}$$

$$s=-\frac{T}{16}\left[\frac{D}{T-1}\right]^2+O\left[\left[\frac{D}{T-1}\right]^4\right]\ . \tag{18}$$

The quality of the squeezed displaced ansatz may be characterized by the square root of the variance (16) itself $(\langle H_{\mathrm{FG}}\rangle-\langle H_{\mathrm{FG}}\rangle^2)^{-1/2}$, which is a measure for the nondiagonality of the variational ansatz. This is shown in Fig. 6. For $D=0$, the trial wave function (14) is an exact eigenfunction of $H^{(-1)}_{\mathrm{FG}}$ with $d=s=0$, i.e., $\phi^{(-1)}_{\mathrm{FG}}(Q)=\phi_0(Q)$. For a fixed value of the transfer parameter T and ascending values of D the energetic uncertainty of the trial wave function increases. For a fixed value of D and ascending values of T the nondiagonality is diminished. Comparing the optimized values for $(\langle H^2_{\mathrm{FG}}\rangle-\langle H_{\mathrm{FG}}\rangle^2)^{1/2}$ with the energetic spacing between two eigenstates, which is in the order of Ω, we conclude that for $D\ll T$ the ansatz (14) yields a rather accurate trial wave function.

Figure 7 depicts the contrast in the functional forms of the lowest conventional state and that of the lowest unconventional state for parity $p=-1$. The squeezed nature of the latter, as contrasted to the undisturbed oscillator function, is shown in Fig. 8. As one realizes, the exact numerical result for the chosen model parameters $(D=15, T=50)$ practically coincides with our optimized trial wave function (14). The energetic uncertainty of the trial state (for $D=15, T=50$) is $(\langle H^2_{\mathrm{FG}}\rangle-\langle H_{\mathrm{FG}}\rangle^2)^{1/2}=0.04\Omega$.

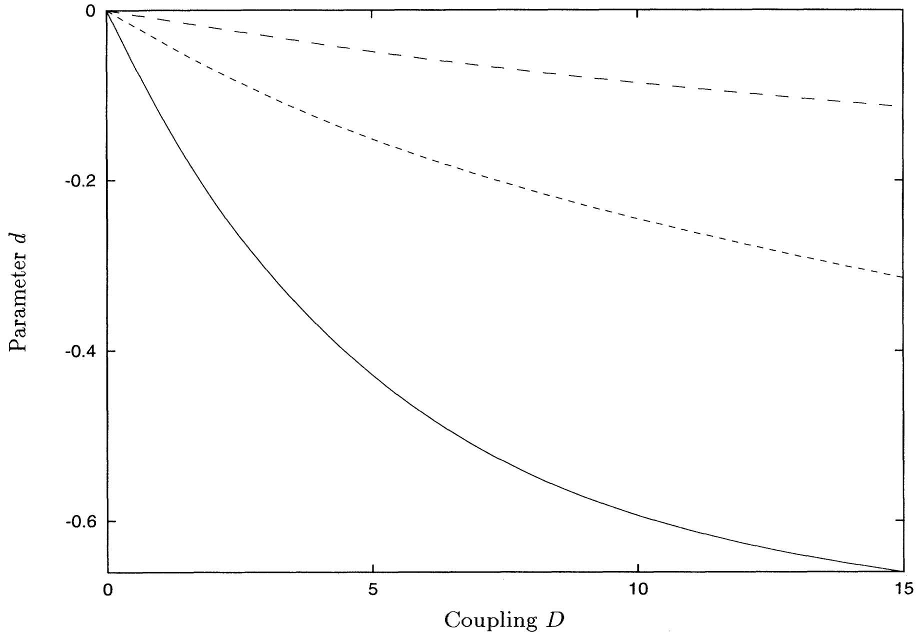

FIG. 4. Optimized variational parameter d of the unitary displacement operator (8) and of the approximate FG wave function (14) for $p=-1$. Solid line: $T=5$, short dashes: $T=15$, long dashes: $T=50$.

IV. ANALYTICAL VERIFICATION OF SQUEEZING: FRÖHLICH TRANSFORMATION

Squeezed oscillatory wave functions are manifestations of a hardening in the effective oscillatory system. Therefore it would be desirable to verify in a direct analytical manner the effective spring hardening which pertains to the nonconventional states. It turns out that this indeed can be demonstrated by means of a Fröhlich-type unitary transformation. The Fröhlich transformation is perhaps the most famous of all unitary transformations. It has been devised originally to establish the effective electron-electron interaction in an originally coupled electron-phonon system.[11] The famous BCS Hamiltonian of superconductivity constitutes a simplified version of the transformed Fröhlich Hamiltonian. The transformation can also be applied to our exciton-phonon Hamiltonian (1). In this case the transformation operator $U_F=\exp(S_F)$ is of a mixed exciton-phonon nature

$$S_F=a(|l\rangle\langle r|-|r\rangle\langle l|)Q+ib(|l\rangle\langle l|-|r\rangle\langle r|)Q$$
$$+c(|l\rangle\langle r|-|r\rangle\langle l|)P+id(|l\rangle\langle l|-|r\rangle\langle r|)P\ , \tag{19}$$

$(a,b,c,d$ real). The terms in S_F are chosen to be linear in

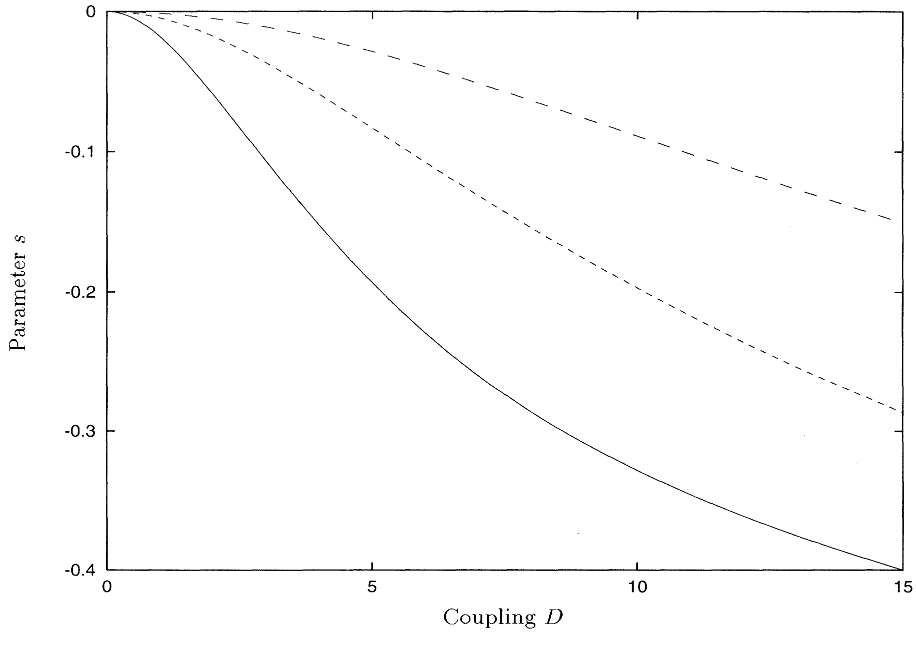

FIG. 5. Optimized variational parameter s of the unitary squeezing operator (9) and of the approximate FG wave function (14) for $p=-1$. Solid line: $T=5$, short dashes: $T=15$, long dashes: $T=50$.

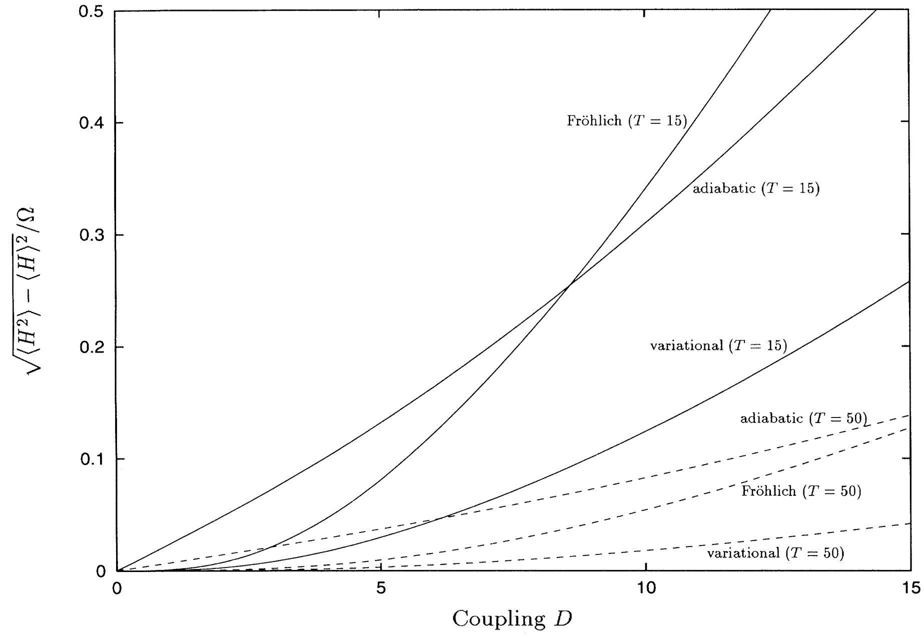

FIG. 6. Energy uncertainty of the *variational* ansatz (14), the approximate wave function (29) deduced by the *Fröhlich*-type transformation and the *adiabatic* wave function (39) for $p=-1$. Solid line: $T=15$, dashed line: $T=50$.

Q or P and to commute with the total reflection operator $R=R_{\text{ex}}R_Q$. Thus, the Fröhlich transformation, as defined by the exponent (19), takes into account the reflection symmetry of the Hamiltonian (1) by $[U_F,R]=0$.

It turns out to be more favorable to proceed first to the FG frame before applying the Fröhlich transformation. For that purpose we employ the unitarity relation $U_{\text{FG}}U_{\text{FG}}^{\dagger}=1$ for the transcription

$$U_{\text{FG}}^{\dagger}(U_F^{\dagger}HU_F)U_{\text{FG}}=\widetilde{U}_F^{\dagger}(U_{\text{FG}}^{\dagger}HU_{\text{FG}})\widetilde{U}_F \tag{20}$$

with the FG transformed Fröhlich operator

$$\widetilde{U}_F=U_{\text{FG}}^{\dagger}U_FU_{\text{FG}} \ . \tag{21}$$

Using the transformation formulas (3) we find that $\widetilde{U}_F$ is diagonal in the excitonic subspace

$$\begin{aligned}\widetilde{U}_F&=\exp\left\{\sum_p |p\rangle\langle p|\widetilde{S}_F^{(p)}(Q,P)\right\} ,\\ \widetilde{S}_F^{(p)}(Q,P)&=paQR_Q+ibQ+pcPR_Q+idP \ ,\end{aligned} \tag{22}$$

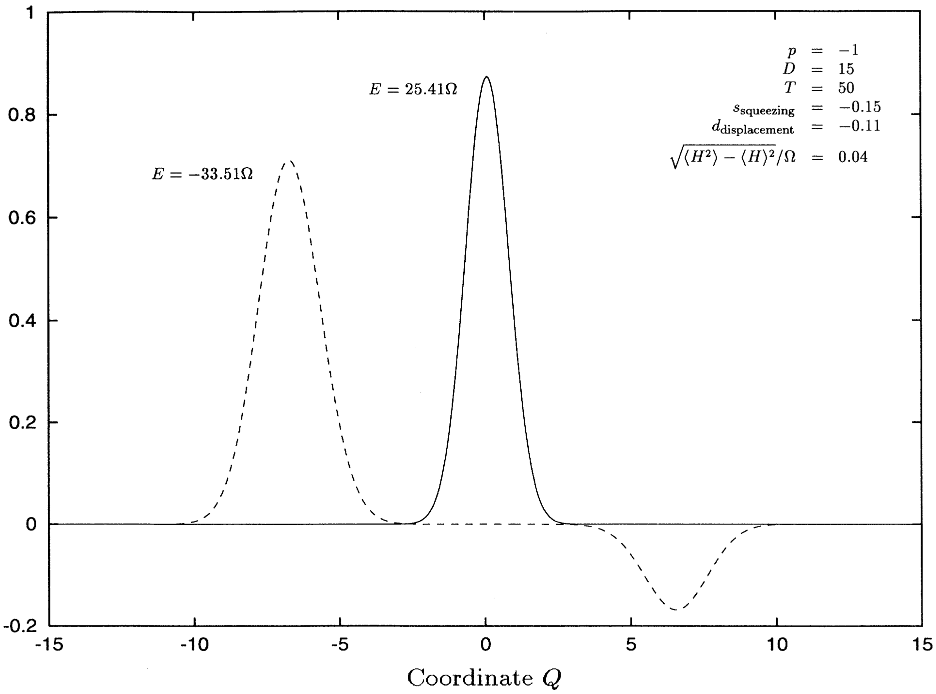

FIG. 7. Contrast in the functional forms of the lowest conventional state (dashed line) and the lowest nonconventional state ("exotic," solid line), represented by the optimized trial wave function (14). Parameter set: $p=-1, D=15, T=50$.

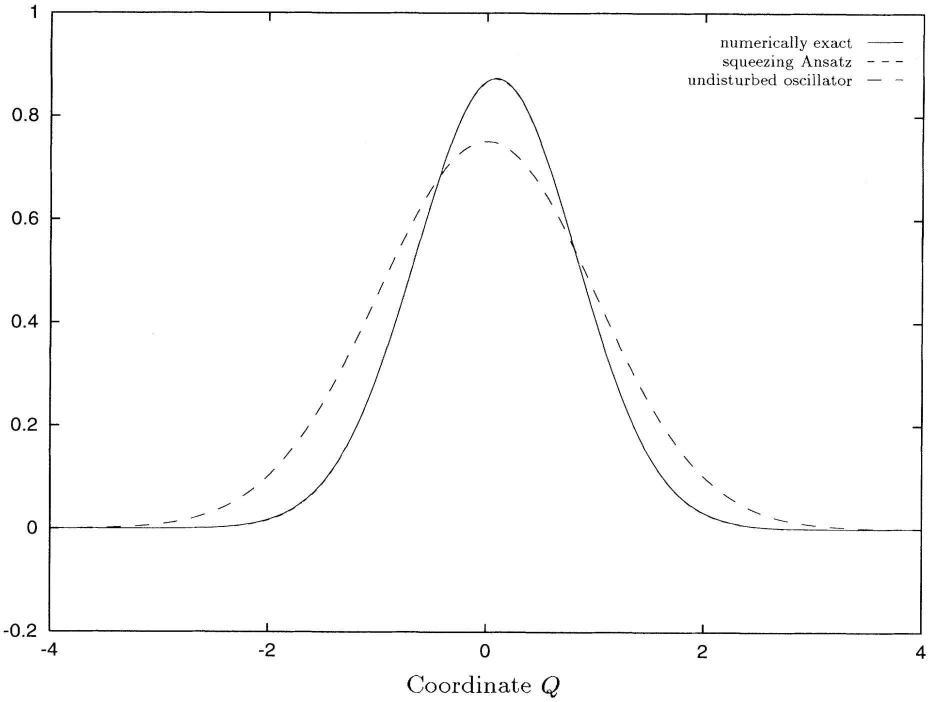

FIG. 8. Comparison of the ground-state wave function of the undisturbed harmonic oscillator (long dashes) with the lowest nonconventional state, represented both by the exact numerical solution of the FG equation (5) (solid line) and by the optimized trial wave function (14) (short dashes). The latter practically coincides with the exact result.

where $\widetilde{S}_F^{(p)}(Q,P)$ pertains to the vibrational subspace only. In order to apply the Fröhlich operator in the FG frame, $\exp(-\widetilde{S}_F^{(p)})H_{\mathrm{FG}}^{(p)}\exp(\widetilde{S}_F^{(p)})$, we split up the FG Hamiltonian into two parts, $H_{\mathrm{FG}}^{(p)}=H_0^{(p)}+W$,

$$H_0^{(p)}=\frac{\Omega}{2}(P^2+Q^2-pTR_Q)\ , \tag{23}$$

$$W=\frac{\Omega}{2}DQ\ . \tag{24}$$

The transformation parameters a to d of (22) are fixed by the Fröhlich condition

$$[H_0^{(p)},\widetilde{S}_F^{(p)}]=-W\ , \tag{25}$$

which yields

$$a=-\frac{DT}{2(T^2-1)}\ ,\quad d=-\frac{D}{2(T^2-1)}\ ,\quad b=c=0\ . \tag{26}$$

The Fröhlich transformed FG Hamiltonian then assumes the form

$$\begin{aligned} e^{-\widetilde{S}_F^{(p)}}H_{\mathrm{FG}}^{(p)}e^{\widetilde{S}_F^{(p)}} &= H_0^{(p)}+\left[\frac{1}{1!}-\frac{1}{2!}\right][W,\widetilde{S}_F^{(p)}]+\left[\frac{1}{2!}-\frac{1}{3!}\right][[W,S_F^{(p)}],\widetilde{S}_F^{(p)}]\cdots \\ &= \frac{\Omega}{2}\left\{P^2+Q^2-pTR_Q+\frac{D^2}{4(T^2-1)}-p\frac{TD^2}{2(T^2-1)}Q^2R_Q \right. \\ &\qquad \left. -\frac{TD^3}{3(T^2-1)^2}(TQ^3+pQR_Q+ipQ^2PR_Q)\right\}+O(D^4)\ . \end{aligned} \tag{27}$$

For the moment we restrict our discussion to the terms up to second order in D. Then the expression (27) displays a reflection symmetry and it has parity-ordered eigenfunctions $\widetilde{\phi}_F^{(p,\pi)}$, where p further pertains to the parity of the full eigenstate (6), whereas $\pi=\pm1$ is the artificial parity of the eigenfunction of (27), which appears if anharmonic terms are neglected. The most interesting term in the transformed Hamiltonian (27) is the Q^2R_Q-term which is a positive or negative correction to the undisturbed Q^2 term depending on the parity $p=\pm1$ of the total wave function and on the parity π of the approximate Q-space wave function $\widetilde{\phi}_F^{(p,\pi)}(Q)=\widetilde{U}_F^\dagger\phi^{(p)}(Q)$.

From Eq. (27) we note that if is applied to $\widetilde{\phi}_F^{(p,\pi)}$ for $p\cdot\pi=-1$, the Q^2 correction term in (27) establishes an increased effective oscillatory frequency which corresponds to an elastic hardening and to a squeezing of the oscillatory wave functions. This situation then would pertain to the unconventional states.

For $p\cdot\pi=+1$ on the other hand, the Q^2 correction term produces an elastic softening and pertains to the states of conventional nature (broadened in Q space). It is worth noting that in this case the correction term tends to compensate the undisturbed Q^2 term and may produce a harmonic instability. It is in this critical range of parameters where the functional form of the conventional states turns from a one-peak (antisqueezed broadened) form to a form with two peaks (mirror images with different weight).[10]

Thus for a fixed value of p we find two distinct sequences of eigenstates, depending on their symmetry properties in Q space. For $p=-1$ the symmetric wave functions ($\pi=+1$, even number of nodes) display a squeezing and their energetic spacing is increased (cf. Fig. 2). The antisymmetric eigenstates ($\pi=-1$, odd number of nodes) are spatially broadened and energetically compressed. For $p=+1$ the situation is reversed.

If we disregard in Hamiltonian (27) the anharmonic terms, the lowest state for $p=-1$ and $\pi=+1$ is a squeezed oscillatory function

$$\begin{aligned}&\tilde{\phi}_F^{(p=-1,\pi=+1)}=(\pi\Omega/\tilde{\Omega})^{-1/4}\exp[-(\tilde{\Omega}/\Omega)Q^2/2]\ ,\\&\tilde{\Omega}=\Omega\{1+[TD^2]/[2(T^2-1)]\}^{1/2}\ .\end{aligned}\tag{28}$$

Reversing the Fröhlich transformation, we find the Fulton-Gouterman wave function $\phi_F^{(p,\pi)}=\tilde{U}_F\tilde{\phi}_F^{(p,\pi)}$

$$\begin{aligned}\phi_F^{(p=-1,\pi=+1)}\approx{}&N^{-1/2}\{1-[a+(\tilde{\Omega}/\Omega)d]Q\}\\&\times\exp[-(\tilde{\Omega}/\Omega)Q^2/2]\ ,\end{aligned}\tag{29}$$

$$N=\sqrt{\pi\Omega/\tilde{\Omega}}\{1+[\Omega/(2\tilde{\Omega})][a+(\tilde{\Omega}/\Omega)d]^2\}\ ,$$

which for $D=15$ and $T=50$ practically coincides with the numerically found exact solution of Fig. 8. The nondiagonality of the wave function (29) can be estimated by calculating the variance of the terms of (27), which are of third order in the coupling D. For large transfer rates T, which is the parameter regime we are primarily interested in, the nondiagonality is proportional to $(\langle\phi_F^{(p,\pi)}|Q^6|\phi_F^{(p,\pi)}\rangle)^{1/2}$. The results are shown in Fig. 6.

Contrasting the approach via the trial wave function of Sec. III and the Fröhlich approach, the main advantage of the latter is that the calculations for the truncated Hamiltonian can be performed analytically. However, a residual problem of the Fröhlich transformation is that the fully transformed Hamiltonian (27) cannot be written down in a closed form. It only can be expressed by an operator series in the coupling constant D.

V. ALTERNATIVE ANALYTIC VERIFICATION OF SQUEEZING

One way out of the aforementioned difficulty is to substitute the transformation operator $\tilde{U}_F=\exp(S_1+S_2)$ by the product $U_1\cdot U_2=\exp(S_1)\cdot\exp(S_2)$, where

$$U_1=e^{S_1}\ ,\quad U_2=e^{S_2}\ ,\quad S_1=paQR_Q\ ,\quad S_2=idP\ .\tag{30}$$

The resulting sequence of transformations is not equivalent to the one given by $\exp(S_1+S_2)$ due to $[S_1,S_2]\neq0$, but choosing the coefficients a and d as defined in (26), the product transformation again satisfies the Fröhlich condition (25). Both the transformation defined by the exponential $\exp(S_1)$ (reflective transformation) as well as the transformation given by $\exp(S_2)$ (displacement transformation in Q space) yield transformation rules for P, Q, and R_Q that can be represented by closed forms ($T_i:A=U_i^\dagger AU_i$),

$$\begin{aligned}&T_1:Q=\cos(2aQ)Q+p\sin(2aQ)QR_Q\ ,\\&T_1:P=\cos(2aQ)P+p\sin(2aQ)PR_Q\\&\qquad\qquad+ia\sin(2aQ)-ipa\cos(2aQ)R_Q\ ,\\&T_1:R_Q=\cos(2aQ)R_Q-p\sin(2aQ)\ ,\\&T_2:Q=Q-d\ ,\\&T_2:P=P\ ,\\&T_2:R_Q=R_Qe^{2idP}\ .\end{aligned}\tag{31}$$

The transformed FG Hamiltonian then reads

$$\begin{aligned}U_2^\dagger U_1^\dagger H_{\mathrm{FG}}^{(p)}U_1U_2=\frac{\Omega}{2}\Big\{&P^2-2ipaPR_Qe^{2idP}+a^2+(Q-d)^2\\&+D\cos[2a(Q-d)](Q-d)+pD\sin[2a(Q-d)](Q-d)R_Qe^{2idP}\\&-pT\cos[2a(Q-d)]R_Qe^{2idP}+T\sin[2a(Q-d)]\Big\}\end{aligned}\tag{32}$$

$$\begin{aligned}\approx\frac{\Omega}{2}\Big\{&P^2+Q^2-pTR_Q+\frac{D^2}{4(T^2-1)}\\&-p\frac{TD^2}{2(T^2-1)}Q^2R_Q+p\frac{TD^2}{2(T^2-1)^2}(Q^2-P^2)R_Q\Big\}+O(D^3)\ .\end{aligned}\tag{33}$$

Comparing the expansion (33) with the harmonic form of (27) we recognize an additional term in (33) which arises from the noncommutativity of S_1 and S_2

$$\frac{1}{2}[H_0,[S_1,S_2]]=p\frac{TD^2}{2(T^2-1)^2}(Q^2-P^2)R_Q\ .\tag{34}$$

If we neglect the anharmonic terms the transformed Hamiltonian (32) for $p=-1$ is diagonal with respect to the symmetric wave function ($\pi=+1$)

$$\bar{\phi}^{(p=-1,\pi=+1)}_{U_1U_2}=(\pi\Omega/\bar{\Omega})^{-1/4}\exp[-(\bar{\Omega}/\Omega)Q^2/2] \ , \tag{35}$$

$$\bar{\Omega}=\Omega\left\{\frac{2(T^2-1)^2+TD^2(T^2-1)-TD^2}{2(T^2-1)^2+TD^2}\right\}^{1/2} . \tag{36}$$

In the FG space the wave function $\phi^{(p,\pi)}_{U_1U_2}=U_1U_2\bar{\phi}^{(p,\pi)}_{U_1U_2}$ then assumes the form

$$\phi^{(p=-1,\pi=+1)}_{U_1U_2}=(\pi\Omega/\bar{\Omega})^{-1/4}\left\{\cos(aQ)\exp[-(\bar{\Omega}/\Omega)(Q+d)^2/2]\right. \tag{37}$$

$$\left.-\sin(aQ)\exp[-(\bar{\Omega}/\Omega)(Q-d)^2/2]\right\} . \tag{38}$$

For the case of a large transfer parameter T the results of the product transformation and that of the Fröhlich transformation are practically identical because the additional term (34) appearing in the expression (33) is smaller than the first Q^2R_Q correction term by a factor $(T^2-1)^{-2}\ll 1$.

VI. CONTRASTING FRAME: THE ADIABATIC APPROXIMATION

For the sake of completeness we also demonstrate the description of the states in the frame of the adiabatic or Born-Oppenheimer approximation.[15] In this approach the unconventional states appear as solutions pertaining to the upper adiabatic potential. In a preceding paper[10] the Born-Oppenheimer formalism was discussed in connection with the ground state of the Hamiltonian (1), and we refer to this work for more details.

In the adiabatic approximation it is assumed that the total wave function $|\Psi_{\mathrm{ad}}(x,Q)\rangle$ can be written as a product of the form

$$|\Psi_{\mathrm{ad}}(x,Q)\rangle=|\chi(x,Q)\rangle|\Phi(Q)\rangle \ . \tag{39}$$

The Q-dependent exciton state $|\chi(x,Q)\rangle$ satisfies the "adiabatic" eigenvalue equation

$$\frac{\Omega}{2}\{-T(|l\rangle\langle r|+|r\rangle\langle l|)+DQ(|l\rangle\langle l|-|r\rangle\langle r|)\}|\chi(x,Q)\rangle=W(Q)|\chi(x,Q)\rangle \ , \tag{40}$$

for the solution of which we employ the two forms

$$|\chi_c(x,Q)\rangle=\sin\eta(Q)\cdot|l\rangle+\cos\eta(Q)\cdot|r\rangle \ , \tag{41}$$

$$|\chi_u(x,Q)\rangle=\cos\eta(Q)\cdot|l\rangle-\sin\eta(Q)\cdot|r\rangle \ , \tag{42}$$

resulting in

$$\sin\eta(Q)=(1/2-DQ/2\sqrt{T^2+D^2Q^2})^{1/2}$$
$$\cos\eta(Q)=(1/2+DQ/2\sqrt{T^2+D^2Q^2})^{1/2} \ . \tag{43}$$

The Q-dependent eigenvalues $W(Q)$ are given by

$$W_{c,u}(Q)=\mp\frac{\Omega}{2}\sqrt{T^2+D^2Q^2} \ , \tag{44}$$

where the minus sign is assigned to the subscript c (conventional) and the plus sign to the subscript u (unconventional). The oscillatory function $|\Phi(Q)\rangle$ is defined by the equation

$$\left[\frac{\Omega}{2}P^2+V^{\mathrm{ad}}_{c,u}(Q)\right]|\Phi_{c,u}(Q)\rangle=\tilde{E}^{\mathrm{ad}}|\Phi_{c,u}(Q)\rangle \tag{45}$$

with the adiabatic potential

$$V^{\mathrm{ad}}_{c,u}(Q)=\frac{\Omega}{2}Q^2+W_{c,u}(Q) \ . \tag{46}$$

Due to the inversion symmetry of $V^{\mathrm{ad}}_{c,u}(Q)$, Eq. (45) has parity-ordered eigenfunctions $|\Phi^{(\pi)}_{c,u}(Q)\rangle$

$$R_Q|\Phi^{(\pi)}_{c,u}(Q)\rangle=\pi|\Phi^{(\pi)}_{c,u}(Q)\rangle \ , \quad \pi=\pm 1 \ . \tag{47}$$

In Fig. 9 the potentials $V^{\mathrm{ad}}_{c,u}(Q)$ are depicted for various values of D and a fixed T. It is evident that for $D>0$ the upper adiabatic potential $V^{\mathrm{ad}}_{u}(Q)$ corresponds to a compressed parabola and its eigenfunctions can be roughly approximated by squeezed versions of harmonic oscillator wave functions.

From Eq. (43) we note the symmetry relation $R_Q\sin\eta(Q)=\cos\eta(Q)R_Q$. Then a comparison of the total wave function (6) and the adiabatic ansatz (39) with (42) reveals that the exact FG wave functions $|\phi^{(p)}\rangle$ for the unconventional states can be approximated by the adiabatic oscillatory wave functions $|\Phi^{(\pi)}_{u}(Q)\rangle$ via

$$\frac{1}{\sqrt{2}}|\phi^{(p=-\pi)}\rangle\approx\cos\eta(Q)\cdot|\Phi^{(\pi)}_{u}(Q)\rangle \ . \tag{48}$$

The connection between the parity p of the exact total wave function [cf. Eq. (6)] and the parity of the adiabatic oscillatory wave function $|\Phi^{(\pi)}_{u}(Q)\rangle$ is established by $p=-\pi$. Thus the eigenfunctions of (45) which have an even number of nodes and which pertain to the upper

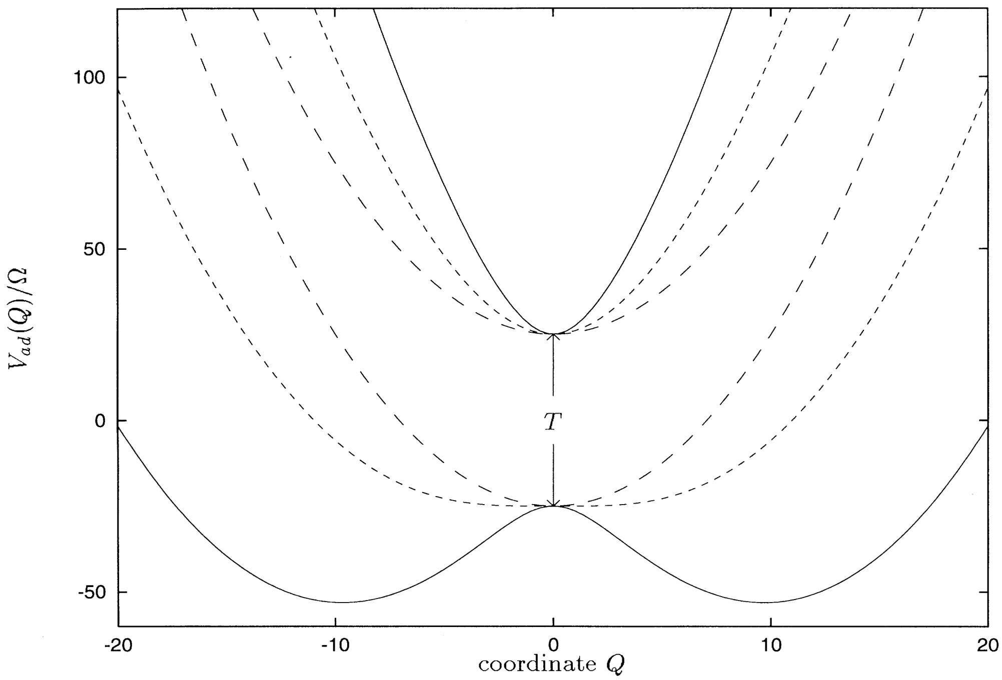

FIG. 9. Adiabatic potentials $V_c^{\mathrm{ad}}(Q)$ and $V_u^{\mathrm{ad}}(Q)$ [see Eq. (46)] for fixed transfer $T=50$ and the coupling constants $D=0$ (long dashes), $D=10$ (short dashes), $D=20$ (solid line). For finite D the upper adiabatic potential approximately corresponds to a squeezed parabola and its squeezed eigenstates are connected with the nonconventional states.

adiabatic potential are approximative forms of the unconventional states with parity $p=-1$.

The lowest of these states is calculated by a numerical diagonalization of Eq. (45). From Fig. 6 we recognize that its energetic uncertainty is remarkably larger than that of the optimized trial wave function (14), what is even true for large transfer parameters T, as also noted from Fig. 6. This is caused by the fact that the nonadiabatic contributions to the Hamiltonian are centered in the same spatial region as the wave function $|\Phi_u^{(\pi)}(Q)\rangle$. For details about the separation of the Hamiltonian in adiabatic and nonadiabatic parts we refer to Refs. 14 and 16.

VII. SUMMARY AND PERSPECTIVES

In the present investigation we have discussed the excited states of an exciton-phonon system, which plays an archetypal role. This work has been motivated by preceding numerical findings of excited exciton-phonon states of nonconventional nature, which display a squeezing in the vibrational Q space. Our study employs the FG transcription of the original Hamiltonian as a primary step. The further analysis has been done in an analytical manner, using unitary transformations both to establish trial wave functions as well as to transform the vibrational FG Hamiltonian to a form in which the squeezing characteristics appear in a direct way. The accuracy of our analytical approaches has been evaluated by regarding the mean-square uncertainty of the considered states, which turned out to be much smaller than the energetic spacing between the oscillatory levels. In particular we have shown that the corresponding eigenfunctions found by means of an adiabatic approximation lead to a considerably higher energy uncertainty than those of our approach.

The main goal of our work is to probe analytical tools by applying them to the archetype exciton-phonon model. These tools, which can be referred to as "construction of trial wave functions by means of unitary transformations," are hoped to be useful also for the finding of exciton-phonon wave functions in more extended systems. In particular it is the Fröhlich-type of construction, applied in succession to the Fulton-Gouterman transcription, which may be expected to be helpful for finding appropriate exciton-phonon wave functions in the squeezing and antisqueezing regime. This, on the one hand, would allow for a quantitative discussion of the seminal approach introduced by Holstein[17] and used by many researchers,[18,19] in which an adiabatic semiclassical philosophy is adopted. On the other hand, it would permit a direct evaluation of transport quantities in the exciton-phonon system without relying on transport equations and the introduction of semiphenomenological relaxation times for the scattering processes.

---

[1] I. Fugol, Adv. Phys. **37**, 1 (1988).

[2] Ch. B. Lushchik, in *Excitons*, edited by E. I. Rashba and M. D. Sturge (North-Holland, Amsterdam, 1982), p. 505 and references therein.

[3] E. I. Rashba, in *Excitons* (Ref. 2), p. 543.

[4] Y. Toyozawa, in *Electronic Excitations and Interaction Processes in Organic Molecular Aggregates*, edited by P. Reinecker, H. Haken, and H. C. Wolf, Springer Series in Solid State Sciences, Vol. 49 (Springer, Berlin, 1983).

[5] M. Wagner and A. Köngeter, J. Chem. Phys. **88**, 7550 (1988).

[6] R. L. Fulton and M. Gouterman, J. Chem. Phys. **35**, 1059 (1961).

[7] M. Wagner, J. Phys. A **17**, 2319 (1984).
[8] A. Köngeter and M. Wagner, J. Chem. Phys. **92**, 4003 (1990).
[9] H. Eiermann, M. Sonnek, and M. Wagner, J. Lumin. **58**, 47 (1994).
[10] M. Sonnek, Th. Frank, and M. Wagner, Phys. Rev. B **49**, 15 637 (1994).
[11] H. Fröhlich, Proc. R. Soc. A **215**, 291 (1952).
[12] H. B. Shore and L. M. Sander, Phys. Rev. B **7**, 4537 (1973).
[13] H. G. Reik, in *The Dynamical Jahn-Teller Effect in Localized Systems,* edited by Y. E. Perlin and M. Wagner (North-Holland, Amsterdam, 1984).
[14] M. Wagner, *Unitary Transformations in Solid State Physics* (North-Holland, Amsterdam, 1986).
[15] M. Born and J. R. Oppenheimer, Ann. Phys. (Leipzig) **84**, 457 (1927).
[16] M. Wagner, J. Chem. Phys. **82**, 3207 (1985).
[17] T. Holstein, Ann. Phys. **8**, 325 (1959).
[18] D. Emin, Adv. Phys. **22**, 57 (1973).
[19] J. Coste and J. Peyraud, Phys. Rev. B **39**, 13 086 (1989).